DETAILED MODEL DESCRIPTION

Supplementary Materials to:
Allometry of antipredatory jumping on water by water striders

Woojoo Kim[1&], Juliette Amauger[2&], Jungmoon Ha[1], Thai Pham Hong[3,4], Anh Duc Tran[5], Jae Hong Lee[6], Jinseok Park[1], Piotr G. Jablonski[1,7*], Ho-Young Kim[6*], Sang-im Lee[8*]

Affiliations:

[1] Laboratory of Behavioral Ecology and Evolution, School of Biological Sciences, Seoul National University, Seoul 08826, Korea
[2] LadHyX, UMR 7646 du CNRS, École Polytechnique, 91128 Palaiseau, France
[3] Mientrung Institute for Scientific Research (MISR), Vietnam National Museum of Nature, Vietnam Academy of Science and Technology (VAST), 321 Huynh Thuc Khang St, Hue, Vietnam
[4] Graduate University of Science and Technology, VAST, 18 Hoang Quoc Viet, Cau Giay, Hanoi, Vietnam
[5] Department of Applied Zoology, Faculty of Biology, University of Science, Vietnam National University, Hanoi, 334 Nguyen Trai, Thanh Xuan, Hanoi, Vietnam
[6] Department of Mechanical Engineering, Seoul National University, Seoul 08826, Korea
[7] Museum and Institute of Zoology, Polish Academy of Sciences, Wilcza 64, 00-679 Warsaw, Poland
[8] Laboratory of Integrative Animal Ecology, Department of New Biology, DGIST, Korea

*Correspondence to (alphabetically): piotrjab@behecolpiotrsangim.org (P. G. J.), hyk@snu.ac.kr (H.-Y. K.), and sangim@dgist.ac.kr (S.-i.L.)

[&] these authors equally contributed to the work

This is a self-contained description of the core mathematical model for jumping of large water striders. It contains a brief essential technical description of the main theoretical components of the model. The figure numbering is separate in this document, and it includes letter "**M**" to mark that the figure belongs to the supplementary **M**odel description.

Detailed description of the mathematical model of jumping

I. Introduction

The mechanics of jumping of mid-sized Palearctic water striders, such as *Gerris latiabdominis, G. gracilicornis, Aquarius remigis* and *A. paludum* (Fig. M1a) on water has been previously studied[1]. It has been shown that their leg stroke speeds are optimized to maximize their jumping speed and minimize time to take off given their mass and leg length[2], and that individual water strider are able to adjust their angular velocity of midlegs based on previous jumping experience[3]. By pressing the water surface until just before it breaks under water strider legs, these typically studied water striders make a full use of capillary forces that the water surface provides.

Water strider legs may be approximated as long thin cylinders (see also Supplementary Materials Part 7: Fig. S10 for link to empirically measured leg diameter and length**)**. The surface is pierced when a very thin cylinder of a radius $r \ll l_c$ is pressed downward against the water surface in a quasi-static manner to a distance of the order of the capillary length $l_c = [\sigma/(\rho g)]^{1/2}$ with σ and ρ respectively being the surface tension coefficient and density of water, and g being the gravitational acceleration. When the legs sink into the water surface, the drag forces act on the legs, which are significantly smaller than the capillary forces for the mid-sized striders.

While the mid-sized water striders do not break water surfaces for efficient jumps, the larger species such as *Gigantometra gigas* (Fig. M1b) do not follow the aforementioned rule of motion in jumping. *G. gigas* is up to ten times heavier than mid-sized water striders in leg length. Typical mass and middle leg length of *G. gracilicornis* (Fig. M1a) are respectively 30 mg and 20 mm, whereas the giant water striders are up to 500 mg and 100 mm for *Gigantometra gigas* (Fig. M1b). Figure M2 shows a sequence of the jump of a *G. gigas* on water taken by a high-speed camera in a field experiment. We see that the middle legs pierce the water surface to a significant degree, which is not observed for mid-sized striders. Here, we describe the kinematic models of the two pairs of legs separately, and combine the models to predict the jump dynamics of the *G. gigas* and other water striders with similar jumping behavior.

Fig. M1. Two different-sized water striders and basic parameters. (a) A mid-sized water strider, *Gerris gracilicornis*. (b) A gigantic water strider, *Gigantometra gigas*. (c) A side view of a *G. gigas* during its jump with parameters used in the theoretical model.

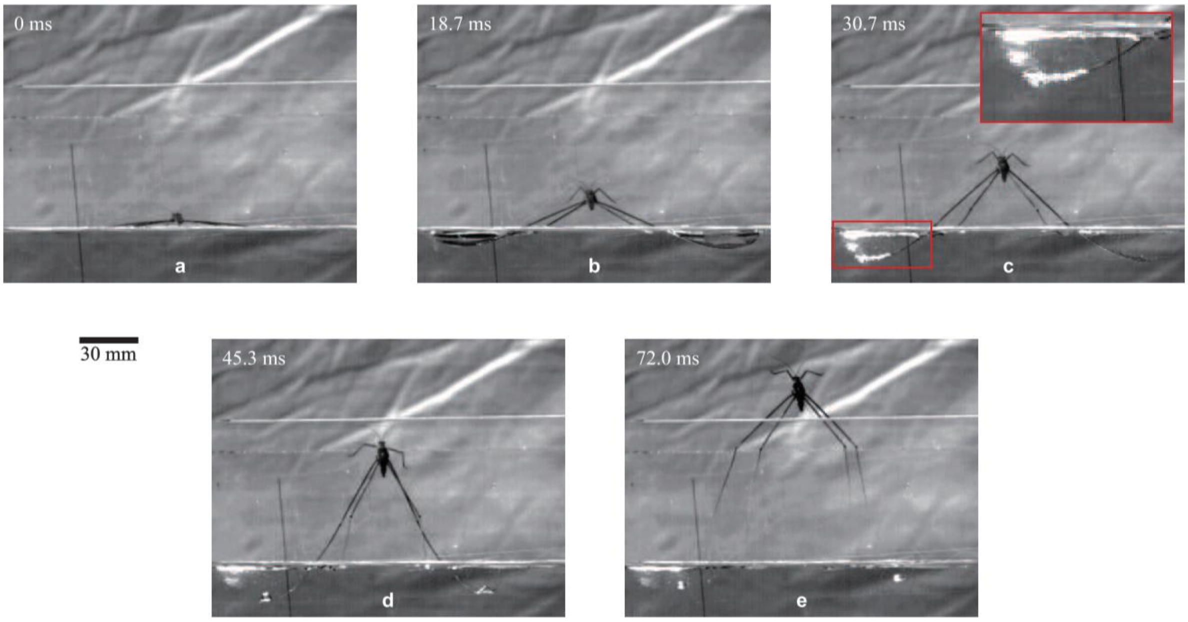

Fig. M2. A sequence of the jump of *G. gigas* on water. (a) The initial posture of the *G. gigas* before jumping. (b) Surface tension phase. The middle and hind legs create dimples on the water surface. (c) The early stage in the drag phase. The middle legs break the water surface with air bubbles covering the legs (magnified image) until they reach the deepest location. (d) The late stage in the drag phase. The air bubbles surrounding the middle legs are absent. (e) Gravity driven phase. All the legs are completely disengaged from the water surface.

II. Kinematics of middle and hind legs

First, we consider the kinematics of middle legs. We assume that their movements comprise two phases: the surface tension phase and the drag phase. In the surface tension phase, the middle legs push the water surface down with a constant wetted length, l_m (the length of tibia plus tarsus of the middle leg). The dimple depth generated by the middle leg, h, grows, leading to the increase of the body center height, y, with time, t (Fig. M1c). As the angular velocity of midleg's downward rotation can be approximated to be a constant, ω[1], the downward linear velocity of the middle leg relative to the body center, v_m, can be written as:

$$v_m = \dot{l_s} = \omega(l_l - y_i)\sin(2\omega t), \qquad (1)$$

where $l_s = y + h$ is the vertical distance from the body center to the tip of the leg. l_l is the entire length of the leg consisting of femur, tibia, and tarsus, and y_i is the initial height of the body centre from the undisturbed free surface. Integrating v_m over time, t, gives:

$$l_s = \frac{1}{2}(l_l - y_i)[1 - \cos(2\omega t)] + y_i \text{ for } l_s = y_i \text{ at } t = 0. \qquad (2)$$

Based on empirical leg measurements, we model the wetted middle legs as cylinders of diameter, d, and length, l_m, according to the details described in the Supplementary Materials PART 7. The water surface cannot withstand the depression of cylindrical legs when the dimple reaches a critical depth, h_c, which was assumed to be 5.4 mm as twice of capillary length, l_c. When the dimple depth, $h = l_s - y$, exceeds h_c at time t_c, in the model, then the wetted part of the middle leg pierces the water surface, entering the drag phase. In this phase, the middle legs are considered almost straight with the wetted length decreasing according to formula:

$$l_1 = l_l - \frac{y}{\cos\left(\frac{\pi}{2} - \omega t\right)}, \qquad (3)$$

that takes into account the ascent of the insect body. The downward linear velocity of a middle leg relative to the water surface is then given by:

$$v_l = \omega(l_l - y_i)\sin(2\omega t) - \dot{y}. \qquad (4)$$

Because the legs penetrate the water with a high velocity, an air bubble forms around the leg, as shown in Fig. M2c. We assume in the model that the air bubble detaches after the moment when the middle legs reach the deepest point in the water. Thus, the effective frontal area, the projected area of the leg with its diameter, d, along its moving velocity, is $A_f = d_b l_1$, thanks to the presence of an air bubble that increases the cylindrical leg diameter, to d_b ("b" stand for bubble of air) by the factor of 3.34 times (d_b=3.44*d) as determined in empirical measurements (see Supplementary Materials PART 7: Table. S7).

We turn to the kinematics of hind legs which do not pierce the water surface during the jump. The stroke can be decomposed into two phases. In the first (pushing) phase, the hindlegs push the water surface down with a fully contacted constant wetted length, l_h (the length of tibia plus tarsus of the hind leg), with a growing dimple depth. We assume in the model that the depth of dimple created by a hind leg from the undisturbed free surface, h_h, grows at the same rate as dimple of the midleg until it reaches constant depth, h_{hm}. Constant depth of hindlegs is calculated using observed empirical maximum depth of hindlegs, h_{hE}, and wetted length of hindlegs assuming leg as half of an arc (see details in Supplementary Materials PART 9).

In the second (drag) phase, which starts when the dimple depth reaches its constant, h_{hm}, the legs slide on the water surface towards the body while detaching themselves from the surface. Thus, the wetted length decreases while the dimple depth is constant. We calculate the wetted length of a hind leg, l_2, based on body heights, y, constant wetted length of a hind leg, l_h, and femur length of a hind leg, l_{Hfemur}. We use a simplifying assumption that the hindlegs that are out of the water align with femur along the direction of jump and are being dragged out from the water surface vertically (Fig. M3, Supplementary Movie 1), while the hindleg section on the water surface is bent creating a dimple without surface breaking. Therefore, the wetted length of a hind leg approximately follows:

$$l_2 = l_h - (y - l_{Hfemur}) \text{ when } y > l_{Hfemur} \text{ and } l_h > (y(t) - l_{Hfemur}). \quad (5)$$

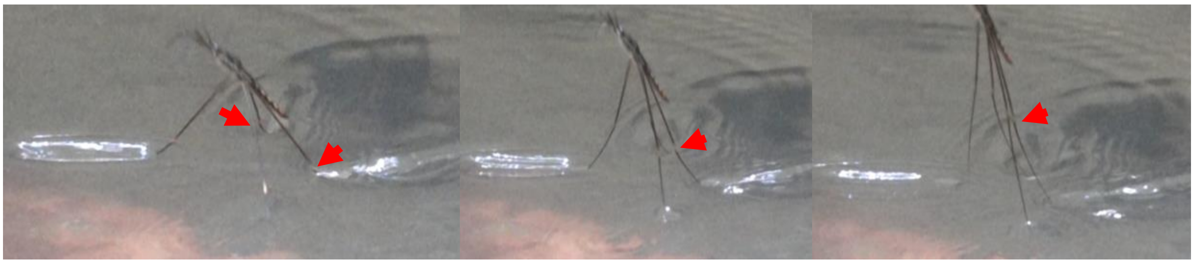

Fig. M3. Field jump of *G. gigas*. Field jump of *G. gigas* shows its hindlegs are almost vertical when the wetted length is pulled out from the water surface. Red arrows mark the femur-tibia joint.

Summarizing the simplified kinematics of both middle and hind legs in the model, we schematically plot the timeline of different phases of the jump for the four legs as shown in Fig. M4. In period 0, $t = 0$, both middle and hindlegs are in stationary situation with initial dimple depth, h_o. In period I, $0 < t < t_c$, both the middle and hind legs moving with angular velocity, ω, are pushing the water surface with growing of dimple, and only dimple depth of hind leg, h_h, stops growing when it reaches specific depth, h_{hm}. In period II, $t_c < t < t_f$, where t_f is the moment of take-off the middle legs, after having pierced the water surface, continue moving in water with angular velocity, ω, surrounded by air bubbles. The hind legs are being closed on the water surface with their wetted length being decreased with constant dimple depth, h_{hm}.

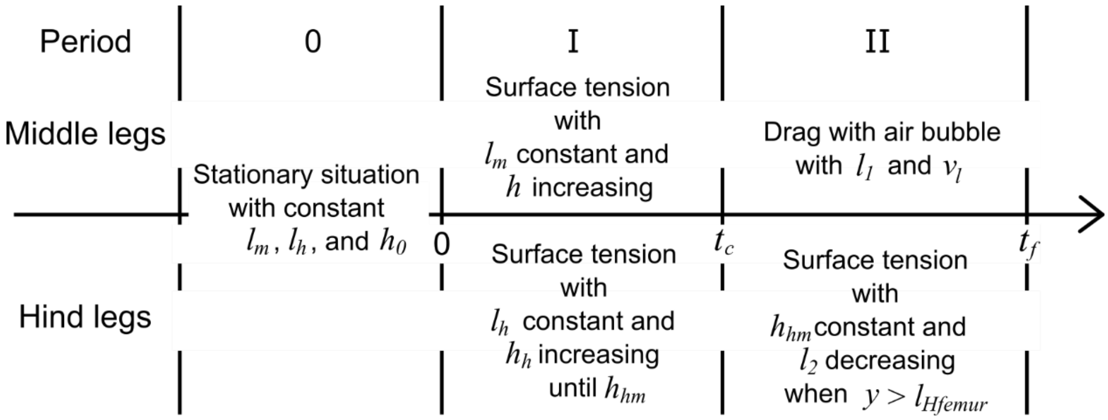

Fig. M4. Timeline of the simulated phases of the jump for the middle and hind legs. Middle and hind legs contribute surface tension force to the jump until the critical moment of time when water surface is broken, t_c. After this moment of time, middle legs of diameter, d_b, resulting from the presence of the air bubble/sheath, create drag force until the moment, t_f. Hindlegs create surface tension force during the whole period from t_c to t_f. This force gradually decreases as the wetted leg length, l_2, decreases, while dimple depth, h_{hm}, is assumed constant.

III. Jump dynamics of *Gigantometra gigas*

The water strider ascends from the water surface because the interaction of its legs and water produces upward thrust. Newton's second law of motion dictates $F = m\ddot{y}$, where F is the total force acting on the water strider legs and m is the water strider mass. We find the temporal evolution of the body center height and the take-off velocity by analyzing the forces produced by the movement of legs of angular velocity, ω.

During the "Period I" (Fig. M4) of the simplified jump, various forces are exerted on the legs including the capillary force $F_c \sim \sigma l_w$, pressure force $F_p \sim \rho U^2 d l_w$, buoyancy $F_b \sim \rho g d h l_w$, added inertia $F_a \sim \rho d^2 l_w U^2/h$, viscous force $F_v \sim \mu r l_w U/l_c$, and the weight of the water strider (for the large *G. gigas* males it is ~ 5 mN). Here, l_w is the wetted leg length, and U is the rate of the vertical growth of dimple, which is a direct consequence of downward linear velocity of the middle leg, v_l that according to formula (4) depends on, among others, on the leg angular velocity, ω.

Using the typical values for middle legs $d = 260$ µm, $l_w = 53.5$ mm, $h = 5$ mm, and $U = 0.4$ ms^{-1}, we found that the capillary force dominates the other forces, and we decided to ignore the other forces in the simplified model.

The capillary force acting on a pair of floating flexible cylinders is given by[2,4]

$$F_c = 4C\rho g l_c l_w h \left[1 - \left(\frac{h}{2l_c}\right)^2\right]^{1/2}, \qquad (6)$$

where C is the flexibility factor depending on the scaled leg length $L_f = l_w/l_e$. Here, $l_e = (Bl_c/\sigma)^{1/4}$ is the modified elastocapillary length of the leg with the bending rigidity $B = \pi E d^4/64$ and E being Young's modulus of insect cuticle. We approximate $C \approx (1 + 0.082L^{3.3})^{-1}$ for $L_f < 2$ and $C \approx (0.88L)^{-1}$ for $L_f > 2$.

We first model the stationary situation, "Period 0" (Fig. M4). We assume the stationary dimple depth of each individual by calculating force balance between gravity and surface tension. When the water strider is on the water surface using their two middle legs and two hind legs, the stationary dimple depth, h_0, satisfies the following formula by assuming the same dimple depth for middle and hind legs:

$$mg = 4\rho g l_c \left\{C_{m0} l_m h_0 \left[1 - \left(\frac{h_0}{2l_c}\right)^2\right]^{1/2} + C_{h0} l_h h_0 \left[1 - \left(\frac{h_0}{2l_c}\right)^2\right]^{1/2}\right\}. \qquad (7)$$

In the surface tension phase, period I, the dimple depth is given by $h = l_s - y$, leading us to write $\ddot{h} = \ddot{l_s} - (F - g)/m$. Here, F is the sum of the capillary forces acting on the middle and hind legs:

$$F = 4\rho g l_c \left\{C_m l_1 h \left[1 - \left(\frac{h}{2l_c}\right)^2\right]^{1/2} + C_h l_2 h_h \left[1 - \left(\frac{h_h}{2l_c}\right)^2\right]^{1/2}\right\}. \qquad (8)$$

This gives a second-order nonlinear differential equation for h with the initial conditions of $h(t = 0) = h_0\ and\ \dot{h}(t = 0) = 0$, which we solve using Matlab. Then we get the body centre height $y = l_s - h$ as a function of time for $0 < t < t_c$ (i.e., $h < h_c$).

Once the middle legs pierce the water surface, $t > t_c$ (i.e., $h > h_c$), the middle legs experience the drag force F_d of water rather than the capillary force. The drag force acting on a pair of middle legs moving with the velocity $v_l = \omega(l_l - y_i)\sin(2\omega t) - \dot{y}$ as obtained above is given by

$$F_d = \rho C_D A_f v_l^2, \qquad (9)$$

where $C_D = 0.8$ is the drag coefficient on the flexible cylinder[5], taken to be about 30% lower than the value for a rigid cylinder at a Reynolds number, $Re = \frac{\rho v_l d}{\mu} \approx 100$. The frontal area is $A_f = d_b l_1$ in period II, $t_c < t < t_f$. Then the total force acting on the middle and hind legs becomes

$$F = \rho C_D A_f v_l^2 + 4C\rho g l_c l_2 h_h \left[1 - \left(\frac{h_h}{2l_c}\right)^2\right]^{1/2}. \qquad (10)$$

Solving $\ddot{y} = (F - g)/m$, a second-order differential equation with A_f, v_l, l_2, h_h being functions of y and t, gives the body center height versus time for period II. The initial conditions are provided from the results of the period I. From the relationship between the body center height versus time we predict time of take-off, t_f, and body speed at v_f. From the body speed and body mass, we predict that maximum jump height above the water surface as $H_m = y_i + \frac{v_f^2}{2g}$ (Supplementary Materials PART 10**)**. These model predictions can be calculated for various vales of angular leg velocities, and for water striders of various body mass and leg lengths.

IV. Explanations of the symbols used in the paper

Explanations of the symbols in the model	
r	Radius of legs as cylinder
σ	Surface tension coefficient of water
ρ	Density of water
g	Gravitational acceleration
$l_c = [\sigma/(\rho g)]^{1/2}$	Capillary length
l_w	Wetted length of the leg
l_l	Entire length of the middle leg consisting of femur, tibia, and tarsus
l_m	Constant wetted length of middle leg (the length of tibia plus tarsus of the middle leg)
l_h	Constant wetted length of hind leg (the length of tibia plus tarsus of the hind leg)
l_{Hfemur}	Femur length of hind leg
l_2	Dynamic wetted length of a hind leg
$l_s = y + h$	Vertical distance from the body center to the tip of the leg
$l_1 = l_l - y/cos(\pi/2 - \omega t)$	Decreased wetted length of middle leg for ascent of the body
$l_e = (Bl_c/\sigma)^{1/4}$	Modified elastocapillary length of the leg
h	Dynamic dimple depth generated by the middle leg
h_c	Critical dimple depth
h_o	Constant dimple depth at stationary situation
h_h	Dynamic dimple depth created by a hind leg
h_{hE}	Maximum dimple depth of hind leg by empirical observations
h_{hm}	Constant dimple depth of hind leg derived from h_{hE}
t	Time
t_c	Critical moment of water surface breaking
t_f	Moment of take-off
y	Body center location on vertical coordinate axis
$\dot{y}$	Time derivative of y in Newtonian calculus notation; vertical speed of body center
y_i	Initial height of the body center from the undisturbed free surface
m	Mass of the water strider
d	Diameter of the wetted middle leg as a cylinder
d_b	Diameter of the wetted middle leg as a cylinder with the air sheath
A_f	Projected area of the leg
ω	Angular velocity of middle leg rotation of a jump
ω_e	Derived angular velocity of middle leg rotation in a jump under the assumption that empirically measured linear downward velocity of wetted midleg relative to water surface, and the vertical distance from the body center can be approximated using a constant value of ω, by two formulae: $v_l = \omega(l_l - y_i)sin(2\omega t) - \dot{y}$, $l_s = \Delta l[1 - \frac{1}{2}\cos(2\omega t) + y_i]$.
ω_t	Hypothetical velocity of midleg rotation of the hypothetical jumps (i.e., surface tension jumps of *G. gigas* and *P. tigrina*; drag-involving jump of *A. paludum*)
v_m	Downward linear velocity of the middle leg relative to the body center
v_f	Take-off velocity
$v_l = \omega(l_l - y_i)sin(2\omega t) - \dot{y}$	Downward linear velocity of a middle leg relative to the water surface
U	Rate of the vertical growth of dimple
μ	Dynamic viscosity
F_c	Capillary force
F_p	pressure force
F_b	Buoyancy
F_a	Added inertia
F_v	Viscous force
$L_f = l_w/l_e$	Scaled leg length
$B = \pi E d^4/64$	Bending rigidity
E	Young's modulus of insect cuticle
C	Flexibility factor; function of wetted length of a leg, l_w, and its bending rigidity, B
C_{m0}	Middle leg flexibility factor; function of wetted length of a middle leg, l_m, and its bending rigidity, B
C_{h0}	Hind leg flexibility factor; function of wetted length of a hind leg,

	l_h, and its bending rigidity, B
C_m	Middle leg flexibility factor; function of wetted length of a middle leg, l_1, and its bending rigidity, B
C_h	Hind leg flexibility factor; function of wetted length of a hind leg, l_2, and its bending rigidity, B
C_D	Drag coefficient
Re	Reynolds number
H_m	Maximum height of the jump
$\Delta l_l = l_l - y_i$	Maximal downward reach of the middle leg
L	Downward stroke; dimensionless maximal reach of the average of four legs
$\Omega = \omega(l_c/g)^{1/2}$	Dimensionless angular velocity of the average four legs' rotation of a jump
$M = m/(\rho l_c^2 C l_w)$	Dimensionless index of insect body mass with respect to the leg; body mass with respect to maximal water mass can be displaced by the average of four legs
$L_m = \Delta l_l / l_c$	Midleg downward stroke; dimensionless maximal reach of the middle leg
$\Omega_\mathrm{m} = \omega_e(l_c/g)^{1/2}$	Dimensionless angular velocity of middle leg rotation of a jump
$M_m = m/(\rho l_c^2 C_{m0} l_m)$	Dimensionless index of insect body mass with respect to the middle leg; body mass with respect to maximal water mass can be displaced by the middle leg

V. Model diagram

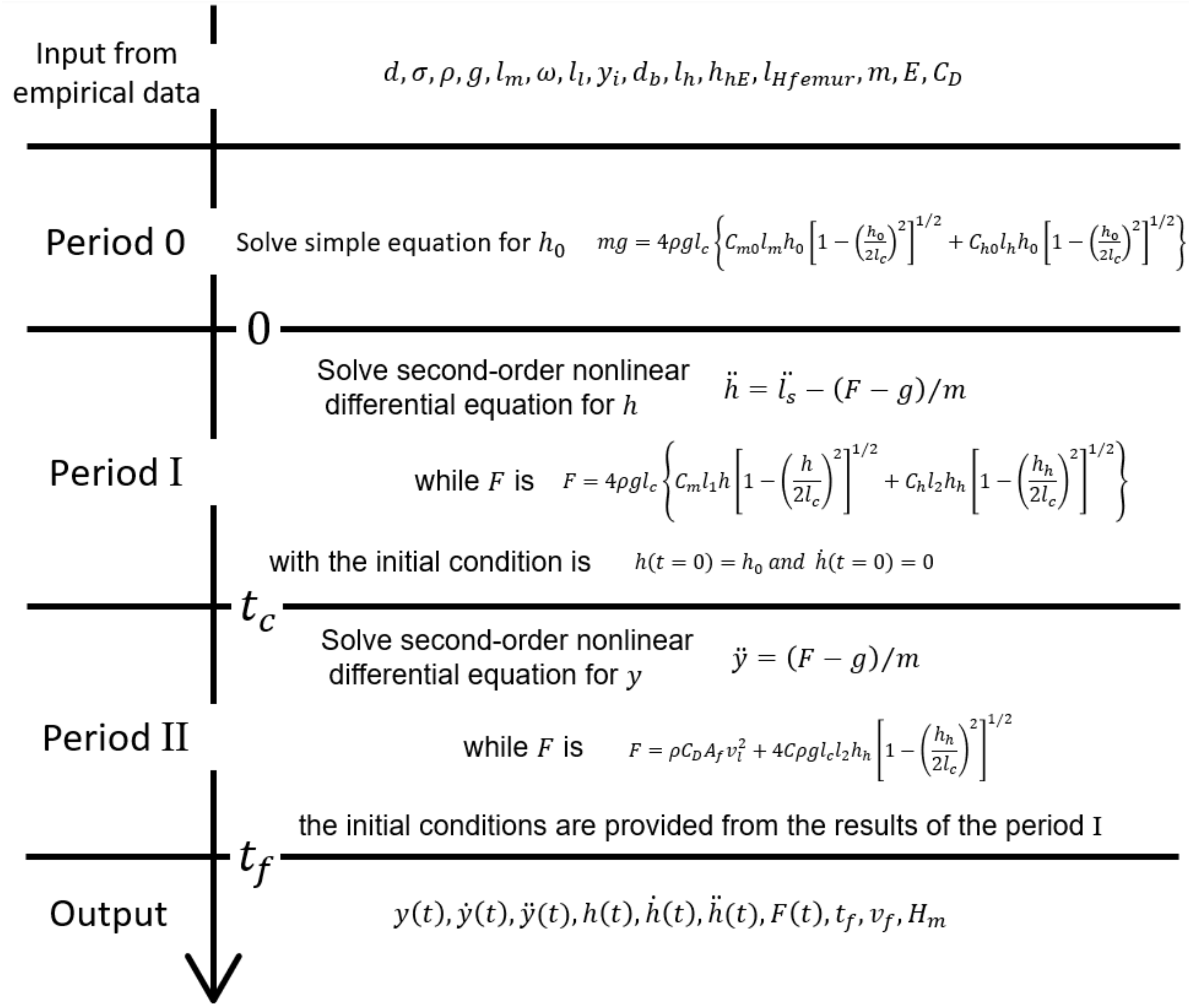

Fig. M5. Simplified diagram of model workflow. After input of the empirical data, in period 0, initial dimple depth, $\boldsymbol{h_o}$, is calculated by solving simple equation for providing initial condition for period I. In period I, $\boldsymbol{h}$, $\boldsymbol{y}$, and $\boldsymbol{F}$ are calculated in the range of $\boldsymbol{0 < t < t_c}$, by solving second-order nonlinear differential equation for $\boldsymbol{h}$. In period II, $\boldsymbol{h}$, $\boldsymbol{y}$, and $\boldsymbol{F}$ are calculated in the range of $\boldsymbol{t_c < t < t_f}$, by solving second-order nonlinear differential equation for $\boldsymbol{y}$. The initial condition of period II is fixed by calculation of period I. Model provides distribution of body height, $\boldsymbol{y}$, dimple depth, $\boldsymbol{h}$, force, $\boldsymbol{F}$, by time and take-off time, $\boldsymbol{t_f}$, take-off velocity, $\boldsymbol{v_f}$, and maximum height, $\boldsymbol{H_m}$. The model simulations were conducted in Matlab. The Matlab code is available at https://doi.org/10.5281/zenodo.7329237.

VI. Values of empirical parameters used in model simulations

Table M1. Empirical parameters used to model jump in each video that has been analyzed in detail.

Parameter/ variable (units)	*G. gigas* male			*G. gigas* female			*P. tigrina*		
	EVT05 (2)	EVT16	EVT41	EVT28	EVT33	EVT35	C0046	C0049	C0066
σ (N/m)	0.072								
ρ (kg/m^3)	998								
g (m/s^2)	9.8								
E (N/m^2)	1e10								
C_D	0.8								
r (m)	11.3e-5	13.1e-5	13.7e-5	11.7e-5	10.4e-5	10.4e-5	7.5e-5	7.5e-5	9.4e-5
ω_e (rad/s)	20	15	16	16	19	17	41	33	29
m (kg)	374.76e-6	483.23e-6	325.41e-6	305.67e-6	226.81e-6	226.81e-6	134e-6	134e-6	123e-6
y_i (m)	0.00017	0.00165	0.00088	0.00333	0.00435	0.00274	0.00271	0.00473	0.00806
l_l (m)	88.64e-3	102.69e-3	103.17e-3	72.59e-3	70.13e-3	70.13e-3	44.72e-3	44.72e-3	50.63e-3
l_m (m)	45.78e-3	54.60e-3	54.05e-3	39.80e-3	38.87e-3	38.87e-3	22.70e-3	22.70e-3	25.56e-3
l_h (m)	63.36e-3	79.48e-3	77.17e-3	44.21e-3	36.98e-3	36.98e-3	16.34e-3	16.34e-3	14.46e-3
l_{Hfemur} (m)	42.74e-3	47.42e-3	48.24e-3	32.25e-3	31.11e-3	31.11e-3	24.30e-3	24.30e-3	28.88e-3
h_{hE} (m)	0.0039	0.0032	0.0062	0.0062			0.0065		
$r_b = d_b/2$	28.5e-5	52.0e-5	48.2e-5	*r**3.34					

Table M2. Empirical parameters used in size-specific simulations.

Parameter/variable (units)	*G. gigas* male	*G. gigas* female	*P. tigrina*	*A. paludum* female
σ (N/m)	0.072			
ρ (kg/m^3)	998			
g (m/s^2)	9.8			
E (N/m^2)	1e10			
C_D	0.8			
r (m)	13.14e-5	11.21e-5	8.934e-5	5.128e-5
m (kg)	413.7e-6	265.2e-6	115.4e-6	47.6e-6
y_i (m)	0.900e-3	0.900e-3	5.17e-3	3.00e-3
l_l (m)	101.9e-3	71.7e-3	47.9e-3	25e-3
l_m (m)	53.5e-3	38.5e-3	23.9e-3	13.4e-3
l_h (m)	73.5e-3	40.6e-3	19.1e-3	9.5e-3
l_{Hfemur} (m)	49.5e-3	32.1e-3	27.6e-3	12.1e-3
h_{hE} (m)	0.0041		0.0065	0.0041
$r_b = d_b/2$	*r**3.34			

References

1. Kim, H.-Y. *et al.* Mechanics of jumping on water. *Phys. Rev. Fluids* **2**, 1–10 (2017).
2. Yang, E., Son, J. H., Lee, S. -i., Jablonski, P. G. & Kim, H.-Y. Water striders adjust leg movement speed to optimize takeoff velocity for their morphology. *Nat. Commun.* **7**, (2016).
3. Baek, M. *et al.* Water strider females use individual experience to adjust jumping behaviour to their weight within physical constraints of water surface tension. *Sci. Rep.* **10**, 1–12 (2020).
4. Vella, D. Floating objects with finite resistance to bending. *Langmuir* **24**, 8701–8706 (2008).
5. Subramanian, C. S., Gurram, H., Kanherkar, P. L., A CFD and experimental study of thin flexible wire in a cross flow. in *Proc. 3rd Int. Conf. Fluid Flow, Heat and Mass Transfer, Ottawa, Canada* (2016).